ACS APPLIED MATERIALS & INTERFACES

Letter

www.acsami.org

Double-Layer Electrode Based on TiO_2 Nanotubes Arrays for Enhancing Photovoltaic Properties in Dye-Sensitized Solar Cells

Zuoli He,[†,‡] Wenxiu Que,*[,†,‡] Peng Sun,[†,‡] and Jiangbo Ren[†,‡]

[†]Electronic Materials Research Laboratory, School of Electronic and Information Engineering, and [‡]International Center for Dielectric Research, Xi'an Jiaotong University, Xi'an 710049, Shaanxi, People's Republic of China

ABSTRACT: The present work reports a rapid and facile method to fabricate a novel double-layer TiO_2 photoanode, which is based on highly ordered TiO_2 nanotube arrays and monodispersive scattering microspheres. This double-layer TiO_2 sphere/TNTA photoanode have got many unique structural and optical properties from TiO_2 scattering microspheres, such as high specific surface area, multiple interparticle scattering, and efficient light-harvesting. Results indicate that this as-fabricated double-layer TiO_2 sphere/TNTA front-illumination dye-sensitized solar cell, which is fabricated from the TiO_2 nanotube arrays with a 17.4 μm length after $TiCl_4$ treatment, exhibits a pronounced power conversion efficiency of 7.24% under an AM1.5 G irradiation, which can be attributed to the increased incident photon-to-current conversion and light-harvesting efficiency.

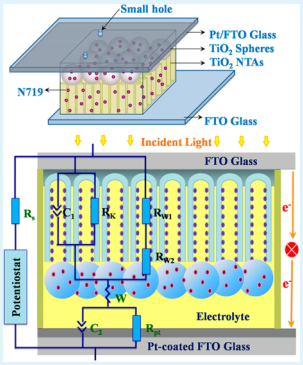

KEYWORDS: *TiO_2, nanotube, array, microsphere, DSSC*

Since dye-sensitized solar cells (DSSCs) were invented by Grätzel in 1991, they have been a cheap and promising alternatives compared to silicon-based solar cells because of their low manufacturing costs, simple fabrication, and high energy conversion efficiencies.[1] Generally, DSSCs were prepared with porous structure TiO_2 nanoparticle film on FTO glass, redox electrolyte (I^-/I^{3-}) and counter electrode (Pt/FTO glass), and the latest energy conversion efficiency of such device, which is based on TiO_2 nanoparticle film and Cobalt (II/III) as redox electrolyte, reached 12.3%.[2] In recent years, many researchers have paid remarkable attention to the synthesis of one-dimensional nanostructures such as nanotube, nanowire, nanobelt, and nanorod and their photovoltaic properties in DSSCs.[3−7] Especially, highly ordered anodic TiO_2 nanotube arrays (TNTAs) can be fabricated by anodic oxidation of Ti foils at low voltage in an aqueous solution containing hydrofluoric acid, offer greatly improved charge collection efficiency due to a high degree of electron mobility along the tube axis with minor charge recombination and high specific surface area from porous TiO_2 nanotubes, which have been confirmed to improve the photovoltaic performances in the DSSCs.[5−7]

Highly ordered anodized TNTAs have attracted remarkable attention for photovoltaic application because of their unique combination of semiconductor properties, nanotube arrays geometrical properties, and electronic transmission characteristics.[7−10] Previous work reported that the morphology and structure of TNTAs can strongly affect the efficiency of charge collection, incident photon-to-current conversion efficiency (IPCE), quantum yield of electron injection, and fill factor (FF) of the DSSCs. Such as $TiCl_4$ surface treatment, removing the caps of the closed bottom, building ordered p−n heterojunction structures, doping metal or nonmetal elements, sensitizing were confirmed to be effective methods for enhancing the efficiency.[7,9−11] Lin introduced the opened-end TNTA-based DSSCs, which exhibited an increase in one-sun power conversion efficiency from 5.3 to 9.1%, corresponding to 70% enhancement as compared to the closed-end ones.[9] Specially, surface treatment using $TiCl_4$ solution results in an increased surface area, charge separation efficiency, photogenerated current and fill factor, ultimately, a higher power conversion efficiency of DSSCs.[11,12] It is noteworthy that the improved transport and electron collection efficiency of the photoanode containing one-dimensional nanostructures alone does not guarantee a high device efficiency. This is because the one-dimensional nanostructures may have relatively small surface area, consequently, the poor capability for dye-attachment uptake.[13,14] TiO_2 nanotube/nanoparticle composite resulted in substantially higher device efficiency, the improved charge transport and collection by the incorporated one-dimensional nanotubes contributes to the high device performance, in addition to an enhanced light scattering by the nanoparticles.[14] Based on these, we try our best to transfer the unique structural and optical properties of TiO_2 scattering microspheres, such as efficient light-scattering and harvesting, high specific surface area, into the TNTA-based DSSCs, which will provide superior capability for both dye attachment and charge transport.[15]

In this letter, we report TiO_2 scattering microspheres/TNAs as photoelectrode assembles front-illumination dye-sensitized

Received: October 10, 2013
Accepted: December 4, 2013
Published: December 4, 2013

   dx.doi.org/10.1021/am4044745 | *ACS Appl. Mater. Interfaces* 2013, 5, 12779−12783

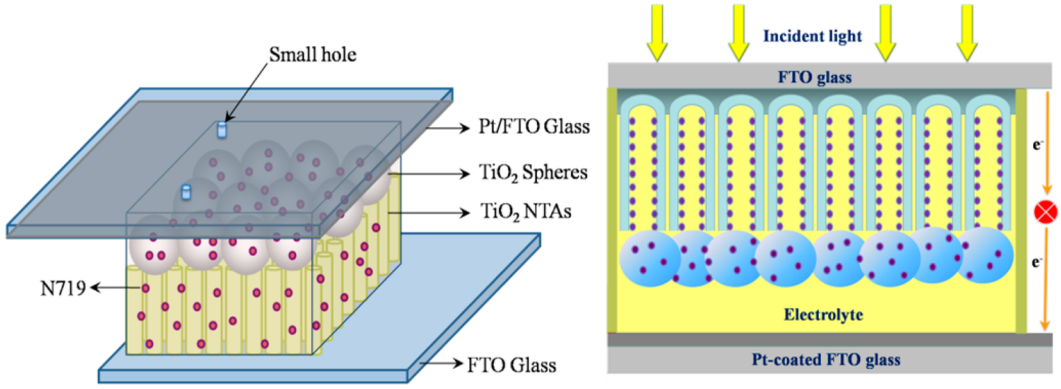

Figure 1. Design scheme for a frontside illuminated TNAs based DSSC.

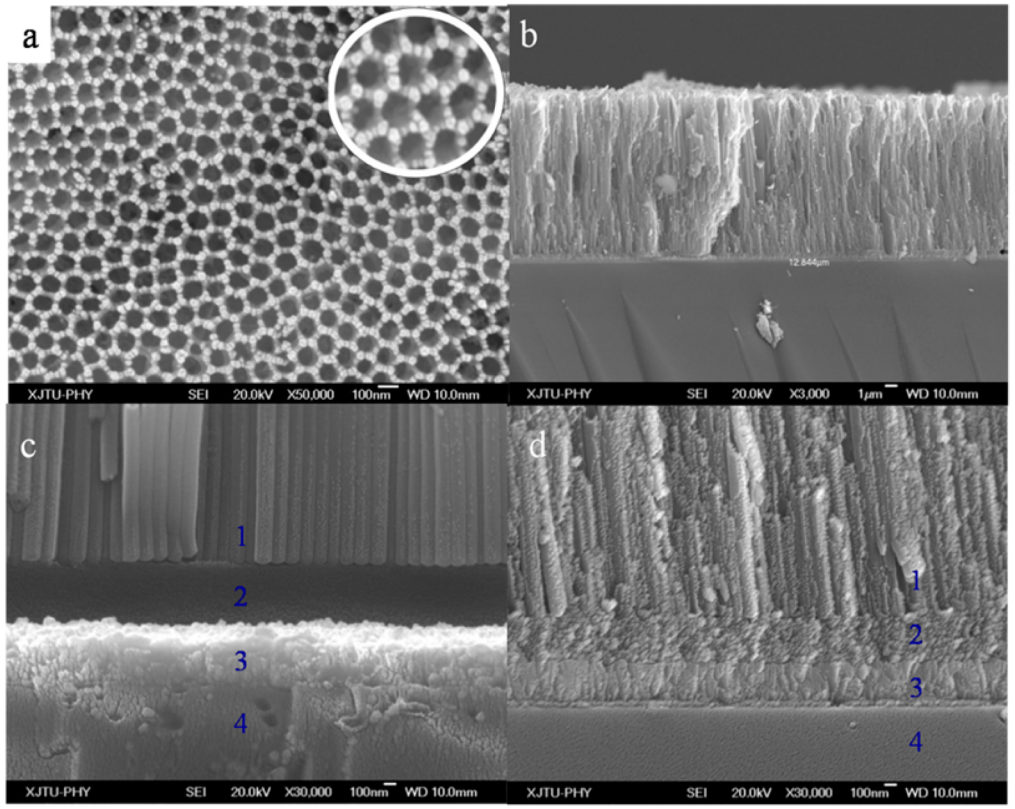

Figure 2. SEM images of highly ordered TiO_2 nanotube arrays: (a) top view; (b) cross-sectional view; (c) cross-sectional view of bottom, before $TiCl_4$ treatment; and (d) cross-sectional view of bottom, after $TiCl_4$ treatment.

solar cells. The photoanode provides multifunction including increased surface area for dye absorption capacity, efficient light-scattering and harvesting. TiO_2 scattering microspheres used in this work were prepared via a microwave solvothermal process and the details on synthesis and properties of the TiO_2 scattering microspheres can be found in our previous research as shown in ref 15.[15] TNTAs were prepared by anodic oxidation of 2 × 5 cm^2 (in size) Ti foils at 50 V in an aqueous solution containing hydrofluoric acid (0.3 wt % NH_4F+ 2 vol % H_2O + glycerol electrolyte). To obtain the free standing TNTA films, we immersed the Ti foils into DI water immediately after anodization. The anodized samples in DI water were bent back and forth until the free standing films were detached from the Ti foils. The detached TNTA films were transferred onto FTO glass with a small drop of TiO_2 sol containing tetra-n-butyl titanate, nitric acid, and polyethylene glycol.[8] Viscous TiO_2 scattering sphere paste prepared by mixing TiO_2 spheres, ethanol, terpinol, and ethyl cellulose coated on the TNTA films with a doctor blade technique. Then, the as-obtained dried TiO_2 sphere/TNTA films were immersed into 40 mM $TiCl_4$ aqueous solution at 70 °C for 30 min, which is expected to improve the photocurrent and photovoltaic performances of the devices. Finally, the as-obtained photoanodes were sintered for 30 min at 500 °C. The schematic structure of the front-illuminated sphere/TNTA-based DSSCs are shown in Figure 1. The as-prepared photoanodes were immersed into a 5 × 10^{-4} M N719 dye solution in a mixture of acetonitrile and tert-butanol (1:1, volume ratio of acetonitrile and tert-butanol) for 24 h. The films and platinized FTO used as counter electrodes were sandwiched together using 60 μm thick heat-sealing film. Followed that the electrolyte (0.03 M I_2, 0.6 M 1-methyl-3-propylimidazolium iodide (PMII), 0.10 M guanidinium

thiocyanate, and 0.5 M tert-butylpyridine in solutions (15:85 volume ratio of valeronitrile and acetonitrile), was injected into the cell from small holes using syring.

Surface morphologies and structures of the as-prepared TNTAs were observed by using a FEI Quatan 250FEG scanning electron microscope (SEM). The anodizing potential and duration were 50 V and 3 h, respectively. SEM images of an anodized Ti foil as represented in Figure 2 clearly show that the TNTAs with 100 nm pore size and 12.3 μm in length have been formed under our present experiment condition. By the way, the TNTAs with the length of 14.6, 17.4, 19.1μm were obtained for an anodization of 4, 5, and 6 h, respectively. The bottoms of the TNTAs before and after $TiCl_4$ treatment are clearly shown in Figure 2c, d, respectively. It can be observed that there are four layers: The top layer is the nanotube array, which its surface is smooth and its outside diameter is about 150 nm; the second layer is the barrier layer about 700 nm thick formed in anodization process; the third one is TiO_2 nanoparticles film formed by TiO_2 sol after annealing, which pastes the TNTA films on FTO and improves the electron transport of the DSSCs; the bottom layer is FTO glass substrate. Obviously, after $TiCl_4$ treatment, these surfaces become rough and many nanoparticles are formed on the surfaces and the space among nanotubes. In addition, the results indicate that there is no destructive damage in the TNTAs during transfer, surface treatment, or annealing.

The performances of the TNTA electrodes in DSSCs were evaluated by sensitizing the electrodes in a 5×10^{-4} M N719 dye solution in a mixture of acetonitrile and tert-butanol (1:1, volume ratio of acetonitrile and tert-butanol) for 24 h, then assembling with platinized FTO used as counter electrodes using heat-sealing film. A liquid electrolyte was injected into interelectrode gap (as shown in Figure 1).[16] The current–voltage (J–V) characteristics of the DSSCs fabricated with the electrodes before or after coating TiO_2 scattering microsphere film layer were measured under an illumination of AM 1.5 solar simulator of 100 mW/cm^2. The current–voltage (J–V) curves for the as-fabricated DSSC cells based on uncoated and sphere-coated TNTA electrodes were shown in Figure 3, and the details of J–V parameters extracted from the J–V curves, such as the J_{SC} , V_{OC}, FF, and the overall conversion efficiency (η), and calculated according to $J_{SC}V_{OC}$FF/(100 mW/cm^2) were present in Table 1. As shown in Figure 3A, the J_{SC} of the 5-TNTA (15.27 mA/cm^2) device is the highest among TNTA DSSCs, and has a conversion efficiency of 6.46%. Correspondingly, after coating the scattering sphere layer, the J_{SC} of the 5-sphere/TNTA device increased to 17.56 mA/cm^2, this enhancement leads to an improved performance in the conversion efficiency, which reaches 7.24%. It also should be noted here that 7.24% is the highest efficiency yet as have achieved in our laboratory by using coating scattering sphere film layer on the TNTA electrode.

Incident photon-to-current conversion efficiency (IPCE) measurements were conducted to analyze the more details of enhanced performance of the DSSCs. Figure 4 displays the IPCE of a TNTA film as a function of wavelength at short circuit.[17] The IPCE is determined by quantum yield of the electron injection, light absorption efficiency of the dye molecules, and efficiency of collecting the injected electrons at the conducting glass substrate, which is strongly affected by the morphology, structure, and the surface area of the photoelectrode.[18] Compared with the untreated TNTA film, the incident monochromatic IPCE spectrum of the TNTA

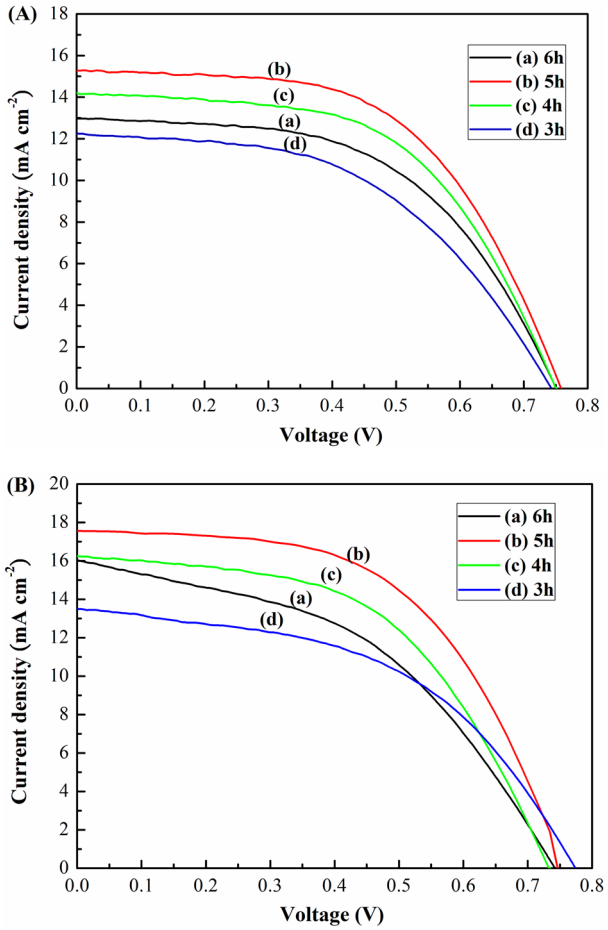

Figure 3. Current–voltage characteristic of the device under AM 1.5 solar simulator 100 mW/cm^2 illumination: (A) before being coated; (B) sphere film after being coated.

Table 1. Photovoltaic Parameters for DSSC Cells Fabricated with Uncoated TNTAs and Sphere-Coated TNTA Electrodes, under AM 1.5 Solar Simulator 100 mW/cm^2 Illumination

photoanode	J_{sc}	V_{oc}	FF	η
3-TNTAs	12.24	0.744	49.9	4.54
4-TNTAs	14.20	0.751	55.4	5.91
5-TNTAs	15.27	0.759	55.7	6.46
6-TNTAs	12.97	0.753	53.5	5.23
3-sphere/TNTAs	13.50	0.772	49.2	5.13
4-sphere/TNTAs	16.25	0.735	52.2	6.23
5-sphere/TNTAs	17.56	0.746	55.3	7.24
6-sphere/TNTAs	16.04	0.744	44.8	5.35

electrode based on the film treated with the $TiCl_4$ shows a maximum of 65.13% for N719. The higher IPCE for the $TiCl_4$ treated film compared with that of the untreated one (57.36%) is attributed to the increased light-harvesting efficiency and the absorption efficiency of the N719 dye molecules at surface of the film, which were brought by $TiCl_4$ treatment. Considering that the anodized TNTAs always have relatively smooth tube walls, hence, the $TiCl_4$ treatment is expected to improve the surface area so that more charge separation interfaces can be created to increase the sunlight absorption, and thus resulting in higher charge-separation efficiency. Actually, TiO_2 nanoparticles can be attached onto both the outer and inner tube

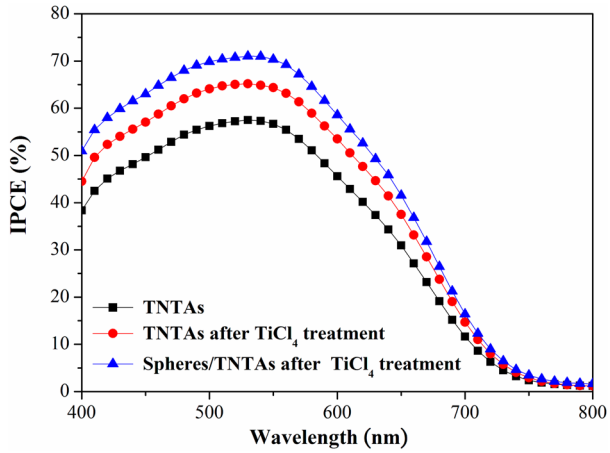

Figure 4. Incident photon-to-current conversion efficiency (IPCE) curves of solar cells based on TNTAs sensitized by N719.

walls to create secondary structures. After such treatment, more dye loading can be expected. Furthermore, the highest IPCE (71.15%) was obtained from the TNTA electrode coated with TiO_2 scattering microsphere film layer before $TiCl_4$ treatment. It should be attributed to the ultrahigh specific surface areas and unique optical properties introduced by the TiO_2 scattering microspheres, which can enhance surface absorption capacity of dye molecules and efficiency of light harvesting and collecting injected electrons at the conducting glass substrate.

Electron impedance spectroscopy (EIS) measurements were performed to investigate the kinetics of charge transfer and recombination in DSSCs, where were using a 10 mV ac on the top of V_{oc} of the DSSC signal in the frequency range of 1×10^{-2} to 1×10^{5} Hz and a potentiostat under an illumination of AM 1.5 solar simulator.[19−21] Figure 5A shows the Nyquist plots of the obtained impedance data of all DSSCs under illumination with AM 1.5 at an applied bias of V_{oc}. Although an equivalent circuit used to fit the experimental data of DSSCs based on spheres/TNTAs is presented in Figure 5B. With changing the conditions, the resistances (R_s, R_1, and R_2) and the capacitances (C_1 and C_2) were changed, so Table 2 presents these fit parameters extracted from the Nyquist plots. The series resistance R_s is caused by the sheet resistance of FTO, current collector contacts, etc.[22] It corresponds to the value in the x-axis where the first semicircle begins.[22,23] The value of R_s changes very slightly, which can be indicated that the $TiCl_4$ treatment or TiO_2 scattering microsphere film layer might have very little relationship with R_s.[23] The resistance R_1 is considered as the sum of interfacial resistance of FTO/TiO_2 and Pt/electrolyte.[20−24] Because the same platinized conducting glass substrate was used as counter electrodes for all DSSCs devices, the value of R_s changes might be caused by the changes in sphere/TNTA or FTO/TNTA interfacial property. The $TiCl_4$-treated one shows the smallest value among the three DSSCs, whereas the scattering microsphere-coated one shows a little increase compared the TNTA-based one (as shown in Figure 5B, the R_{w2} will be introduced in the sphere/TNTA-based DSSCs). The photocurrent density was affected by the charge collection efficiency, which is related to electron lifetime. The resistance R_2 is considered as the sum of the charge transfer resistance at in the TiO_2 film and the dye-absorbed TiO_2/electrolyte interfaces.[22] Therefore, the change in photocurrent density with structures might be related to electron-transport properties. So, it should be noted here the transport resistance

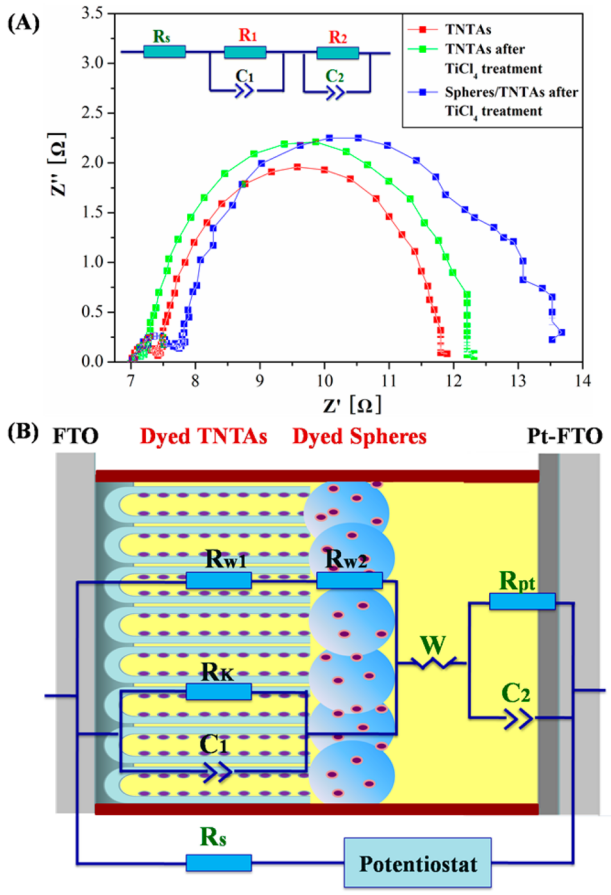

Figure 5. (A) Nyquist plots of the impedance data of the DSSCs; (B) an equivalent circuit used to fit Nyquist plots of the sphere/TNTA-based DSSCs.

Table 2. Summary of Photovoltaic and Photoelectron Transport Properties of DSSCs Based on Various TNTAs and Sphere/TNTA Systems

photoanode	R_s (Ω)	R_1 (Ω)	C_1(F)	R_2 (Ω)	C_2(F)
TNTAs	7.227	0.425	1.967×10^{-3}	4.412	7.390×10^{-3}
TNTAs after $TiCl_4$ treatment	7.095	0.174	4.059×10^{-4}	4.993	7.358×10^{-2}
sphere/TNTAs after $TiCl_4$ treatment	7.324	0.565	6.153×10^{-5}	5.328	1.368×10^{-2}

in sphere/TNTA-based DSSCs will increase, which can be indicated from the increase of R_2. This also further confirms that the increased thickness of the electrode layer could result in the increase in the transport resistance.[22]

In summary, we have developed a method to fabricate a double-layer organized TNTA electrode and we transfer the unique structural and optical properties of TiO_2 scattering microspheres such as efficient light-scattering and harvesting capacity, high specific surface area, and surface adsorption capacity of the dyes into TNTA-based DSSCs. Moreover, the large surface area of the sphere/TNTA film improved light harvesting and dyes adsorption because of the possibility of two layers of adsorbed dye molecules especially the sphere layer, evidenced by the notable photocurrent density and IPCE obtained using the sensitizer N719. The performance of these

double-layer organized TNTA films is markedly improved compared with that of pure TNTA electrodes in dye-sensitized photovoltaic devices, which reveals a way to increase the performance of photovoltaic cells.

AUTHOR INFORMATION

Corresponding Author

*Tel.: +86-29-82668679. Fax: +86-29-82668794. E-mail: wxque@mail.xjtu.edu.cn.

Notes

The authors declare no competing financial interest.

ACKNOWLEDGMENTS

This work was supported by the Research Fund for the Doctoral Program of Higher Education of China under Grant 20120201130004, the National Natural Science Foundation of China under Grant 61078058, the Science and Technology Developing Project of Shaanxi Province (2012KW-11) and the Fundamental Research Funds for the Central Universities.

REFERENCES

(1) O'Regan, B.; Grätzel, M. *Nature* **1991**, *353*, 737−740.
(2) Yella, A.; Lee, H. W.; Tsao, H. N.; Yi, C.; Chandiran, A. K.; Nazeeruddin, M. K.; Diau, E. W. D.; Yeh, C. Y.; Zakeeruddin, S. M.; Grätzel, M. *Science* **2011**, *334*, 629−634.
(3) Liu, Z.; Misra, M. *ACS Nano* **2010**, *4* (4), 2196−2200.
(4) Xu, C.; Shin, P. H.; Cao, L.; Wu, J.; Gao, D. *Chem. Mater.* **2010**, *22* (1), 143−148.
(5) Ye, M.; Xin, X.; Lin, C.; Lin, Z. *Nano Lett.* **2011**, *11* (8), 3214−3220.
(6) Lin, C. J.; Yu, W. Y.; Chien, S. H. *Appl. Phys. Lett.* **2008**, *93*, 133107.
(7) Yan, J.; Zhou, F. *J. Mater. Chem.* **2011**, *21*, 9406−9418.
(8) Lei, B. X.; Liao, J. Y.; Zhang, R.; Wang, J.; Su, C. Y.; Kuang, D. B. *J. Phys. Chem. C* **2010**, *114* (35), 15228−15233.
(9) Lin, C. J.; Yu, W. Y.; Chien, S. H. *J. Mater. Chem.* **2010**, *20*, 1073−1077.
(10) Mohamed, A. E. R.; Rohani, S. *Energy Environ. Sci.* **2011**, *4*, 1065−1086.
(11) Wang, J.; Lin, Z. Q. *Chem. Mater.* **2010**, *22* (2), 579−584.
(12) Sommeling, P. M.; O'Regan, B. C.; Haswell, R. R.; Smit, H. J. P.; Bakker, N. J.; Smits, J. J. T.; Kroon, J. M.; van Roosmalen, J. A. M. *J. Phys. Chem. B* **2006**, *110*, 19191−19197.
(13) Chen, J.; Li, B.; Zheng, J.; Jia, S.; Zhao, J.; Jing, H.; Zhu, Z. *J. Phys. Chem. C* **2011**, *115* (14), 7104−7113.
(14) Alivov, Y.; Fan, Z. Y. *Appl. Phys. Lett.* **2009**, *95*, 063504.
(15) He, Z.; Que, W. *Phys. Chem. Chem. Phys.* **2013**, *15*, 16768−16733.
(16) Kim, H.N.; Moon, J. H. *ACS Appl. Mater. Interfaces* **2012**, *4* (11), 5821−5825.
(17) Park, N. G.; van de Lagemaat, J.; Frank, A. J. *J. Phys. Chem. B* **2000**, *104*, 8989−8994.
(18) Hao, Y.; Pei, J.; Wei, Y.; Cao, Y.; Jiao, S.; Zhu, F.; Li, J.; Xu, D. *J. Phys. Chem. C* **2010**, *114* (18), 8622−8625.
(19) Wang, Q.; Moser, J. E.; Grätzel, M. *J. Phys. Chem. B* **2005**, *109*, 14945−14953.
(20) Adachi, M.; Sakamoto, M.; Jiu, J. T.; Ogata, Y.; Isoda, S. *J. Phys. Chem. B* **2006**, *110*, 13872−13880.
(21) Yoo, B.; Kim, K.; Lee, D. K.; Ko, M. J.; Lee, H.; Kim, Y. H.; Kim, W. M.; Park, N. G. *J. Mater. Chem.* **2010**, *20*, 4392−4398.
(22) Rho, C.; Min, J. H.; Suh, J. S. *J. Phys. Chem. C* **2012**, *116*, 7213−7218.
(23) Fabregat-Santiago, F.; Bisquert, J.; Palomares, E.; Otero, L.; Kuang, D.; Zakeeruddin, S. M.; Grätzel, M. *J. Phys. Chem. C* **2007**, *111*, 6550−6560.
(24) Longo, C.; Nogueira, A. F.; De Paoli, M. A. *J. Phys. Chem. B* **2002**, *106*, 5925−5930.